École Polytechnique

Expansion around models for simulating the charge density

June 22, 2024

M2 Internship Report

Muhammed Hüseyin Güneş[†]

Supervisors:

Vitaly Gorelov[†], Matteo Gatti[†], Lucia Reining[†]

[†]*Laboratoire des Solides Irradiés, École Polytechnique*

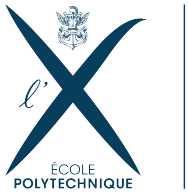

Contents

1 Introduction **2**
1.1 Many-Body Problem 2
1.2 LDA and Nearsightedness 3
1.3 The Benchmark 4
1.4 Defining a new local approximation 5

2 Expanding functionals around models **6**
2.1 Linear response expansion 8
2.2 Motivation from the Cauchy & Lagrange approach 9

3 Connector Theory (COT) **10**
3.1 Local Connector 11
3.2 Bilocal Connector 13

4 Going beyond: expansion around the interacting gas **15**
4.1 Macroscopic contribution to the linear expansion 18

5 Conclusion **21**
5.1 Future Work 21

A Connector Theory: Formalism **22**

B Derivation of the Lindhard Function for the 3D Electron Gas **24**

C Optimizing v_0: exact solution from the HEG **25**
C.1 $\tilde{v}_0$ for the connector 27

1 Introduction

Understanding the effect of interactions between electrons in certain systems, especially crystals, has been of great interest, not only for accurately describing existing systems, but also for the design of new materials with desired properties for many applications such as materials science, semiconductors, and photovoltaics [1, 2]. It is well known that the desired properties of a given system can be described by the laws of quantum mechanics, namely the solutions of the Schrödinger equation. However, solving this equation exactly for systems with more than a few particles quickly becomes impossible due to the computational complexity involved. The wave function is a function of all the coordinates of all the particles in the system, and as the number of particles increases, the number of variables in the wave function grows exponentially. This exponential scaling makes calculations impractical to perform [3].

1.1 Many-Body Problem

Much effort has been put into circumventing this so-called "many-body" problem. These methods include mean-field approximations, such as Hartree-Fock, and more advanced techniques like many-body perturbation theory (MBPT) and density functional theory (DFT), each aiming to approximate the effects of electron-electron interactions in different ways. Central to these methods is the charge density, which plays a crucial role in determining the behavior and properties of interacting particle systems. Charge density provides a spatial distribution of the electronic charge within a system, offering valuable insights into the electronic structure and interactions in different frameworks. It serves as a fundamental quantity because it encapsulates the effects of all electron-electron interactions in a system [3]. Therefore, the accurate determination of charge density is essential for predicting and understanding various physical properties. To effectively utilize charge density, different approaches have been employed. Mean-field approaches, such as the Hartree-Fock method, attempt to approximate the many-body problem by treating the interactions between particles in an averaged way, simplifying the computation of the charge density [2]. Auxiliary systems, like the Kohn-Sham system in Density Functional Theory (DFT), maps the problem of interacting particles onto a system of non-interacting particles that reproduces the same charge density [3].

These methods utilize functionals to express complex many-body interactions in a more manageable form. One of the essential concepts in this context is the nearsightedness. This means that the value of a functional at a specific point is largely determined by the values of the function in a localized region around that point, rather than by the function's behavior far away. This principle reduces the complexity of functional dependencies and makes the calculation of properties much more efficient. In terms of physical applications, nearsightedness implies that the properties of a system at a given point depend primarily on the local environment rather than on distant parts of the system. This was formulated by Walter Kohn in his seminal paper in 1996 [4] and quickly became one of the main successes of DFT. Within the context of DFT,

nearsightedness means the local electronic properties, like the effective potential $v(\mathbf{r})$, depend significantly on the density only at nearby points. Changes of that density, beyond a distance R have limited effects on local electronic properties, which rapidly tend to zero as a function of R.

1.2 LDA and Nearsightedness

This idea of *nearsightedness* naturally led to the formulation of the Local Density Approximation (LDA). LDA assumes that the desired quantity at a point $\mathbf{r}$ solely depends on that point and all the other points have negligible effects on the quantity at $\mathbf{r}$. In the case of DFT, there is only one quantity that is unknown and needs to be approximated: exchange-correlation (xc) energy per particle, ϵ_{xc} from which we describe the total xc energy as,

$$E_{\text{xc}}[n] = \int d\mathbf{r} n(\mathbf{r}) \epsilon_{\text{xc}}(\mathbf{r}, [n])$$

Thus, nearsightedness implies that the unknown term ϵ_{xc}, at every point $\mathbf{r}$, only depends on the density at $\mathbf{r}$. This allows us to neglect all the other points, or assume all the other points have the same density as the point of interest. This describes a well-known system called the homogeneous electron gas (HEG) which has constant density. In other words: at every point $\mathbf{r}$, the exchange-correlation energy is approximated by a homogeneous electron gas that has the density $n(\mathbf{r})$, i.e.

$$E_{\text{xc}}^{\text{LDA}}[n] = \int d\mathbf{r} n(\mathbf{r}) \epsilon_{\text{xc}}^{h}(n(\mathbf{r})) \tag{1}$$

where $\epsilon_{\text{xc}}^{h}(n(\mathbf{r}))$ corresponds to the xc energy of the homogeneous electron gas, already calculated (and stored) from quantum Monte Carlo methods once and for all.

Consequently, LDA successfully leverages tabulated results from a pre-solved model system, such as the Homogeneous Electron Gas (HEG). Considering its significant success and range of applications, this approach serves as a valuable source of inspiration by showcasing how insights gained from a simpler, (numerically) exactly solvable models can be used to approximate more complex real-world systems. Inspired by the principles of LDA, our philosophy in this work is clear: to make extensive use of tabulated results and pre-solved model systems. By employing already solved model systems, we aim to develop efficient methods for calculating properties of real systems. Specifically, we focus on how one can effectively exploit these model systems to calculate charge densities, $n(\mathbf{r})$. This approach not only makes use of recycling existing solutions to reduce computational cost but also provides a robust framework for simulating real systems in a practical and systematic manner. Our main strategy will be to expand our system around the homogeneous electron gas (our model) to simulate the desired quantity in the real system. In Section 2, we start our framework by demonstrating how to expand $n(\mathbf{r})$ (with respect to the effective potential) within the linear regime around a non-interacting electron gas. This will allow us to to bypass solving the Schrödinger

equation while still aiming to achieve results consistent with DFT charge density calculations. In Section 3, we continue this approach and investigate the exactification of nearsighted approximations (such as LDA) by using the Connector Theory (COT) [5] which formulates an exact connection between the real system and any model system by using a mathematical object called the "connector". We shall ask the following question: **Is there a general connector that can yield the exact result in the real system? If yes, what is the systematic approach to obtaining such exact connectors?**. We will see how COT is able to simulate higher order terms in our linear expansion without explicitly calculating them. In Section 4, we will move beyond the non-interacting HEG model and start using the interacting electron gas model. We will demonstrate that this method is a promising path to surpass DFT and move towards the exact regime (since the only ingredient needed is the external potential). Finally, we will provide insights into future work directions and conclude by discussing the broader implications and potential applications of our approach.

1.3 The Benchmark

Throughout our analyses, we select simple cubic Helium (one atom per unit cell) as our system for evaluating results. This choice provides an intriguing test case being far from our model, the homogeneous electron gas. We believe successfully using a homogeneous model to describe such a highly inhomogeneous system will demonstrate the robustness and versatility of our approach. This analysis, therefore, is expected to strengthen the potential of our approach in addressing complex many-body systems, extending its applicability beyond simple models to more intricate real-world scenarios.

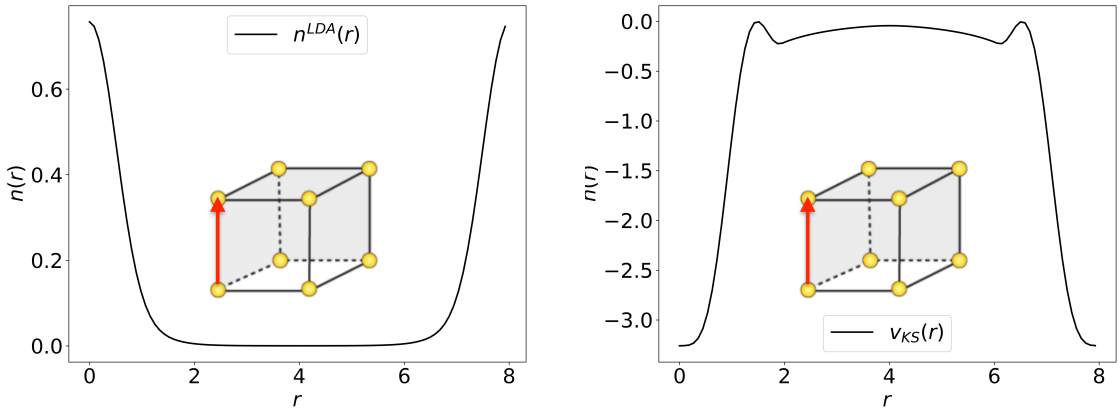

Figure 1: **Left:** Cubic Helium charge density calculated using the DFT-LDA as a function of position in Bohr units. **Right:** Corresponding effective potential, $v_{\mathrm{KS}}(\mathbf{r})$. The plotting trajectory is as shown in the figures, in the z-direction.

Our benchmark consists of two outputs: charge density which will be used as reference, and the Kohn-Sham potential, $v_{\rm KS}(\mathbf{r})$, which we will denote throughout this study as the effective potential and drop the subscript. These two outputs (charge density, $n(\mathbf{r})$ and the effective potential, $v(\mathbf{r})$ are calculated within DFT by using LDA [6]. Therefore they include certain errors. However, for the time being, we shall assume they are exact quantities and see if our methods can achieve consistent results.

1.4 Defining a new local approximation

As stated previously, in the charge density problem, the input is the potential, i.e. $n(\mathbf{r};[v])$. In many cases the situation is reversed, the desired observable is the potential and the input is the density. However, the motivation is the same: To describe the real system, results from a known model system are used and there is a specific quantity connecting the model system to the real one. Within the LDA framework, this corresponds to replacing the exchange-correlation potential at each point with that of a homogeneous electron gas at the density equal to the local density at the point, namely

$$v_{\rm xc}(\mathbf{r},[n]) \approx v^h_{\rm xc}(n(\mathbf{r})) \tag{2}$$

Therefore, the connecting object between the model and the real system is the local density. Here, we use a parallel analogy to define the local potential approximation due to the reversal of pictures. The local potential approximation (LPA) then replaces the density at each point with that of a homogeneous electron gas with a potential equal to the local potential at the point,

$$n(\mathbf{r},[v]) \approx n^h(v(\mathbf{r}))$$

where $v(\mathbf{r})$ is the potential felt by the electrons in the solid. Here, the connecting object between the model and the real system is the local potential (however it may be defined, as we will discuss different possibilities). The model in this case is really simple, it is the well known relation with respect to the Fermi wave-vector, k_F

$$n^h = \frac{k_F^3}{3\pi^2} \tag{3}$$

Since the Fermi energy is defined by the difference between the chemical potential μ and the potential v, we define k_F by the following

$$\mu = \frac{k_F^2}{2} + v \implies k_F = \sqrt{2(\mu - v)} \tag{4}$$

Throughout our study, we set $\mu = 0$ for convenience, i.e. $k_F = \sqrt{-2v}$. From here, we have direct access to LPA, we simply replace the potential at every point as the effective potential

$$n(\mathbf{r}, [v]) \approx n^h(v(\mathbf{r})) = \frac{(-2v(\mathbf{r}))^{3/2}}{3\pi^2} \tag{5}$$

I have tested this approximation for the case of cubic Helium. This is a very tough task because cubic He is very different from the HEG. The result is shown in Figure 2.

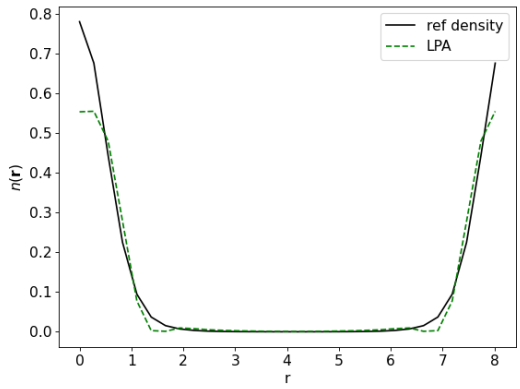

Figure 2: Cubic Helium charge density calculated using the LPA (dashed line) with comparison to the reference density, as a function of position in Bohr units.

As one can see, solely using the simplest model without interactions, we are already able to achieve qualitative agreements with our reference. Even though LPA captures the general behavior of the density (being localized around atoms and vanishing far from atoms), one seeks results with much more accuracy. Moreover, the average number of electrons in a unit cell is overestimated by LPA: it yields $\bar{n} = 2.26$ whereas it should be 2. To try to overcome this problem, a better approach needs to be proposed, rather than making a local approximation. In the next sections, we will see how one can use this approximation as a starting point for expansions, or even exactify it.

2 Expanding functionals around models

In this section, we tackle the problem of expanding functionals around functions. The problem arises when we have a quantity which depends on a function and how to approximate it is not straightforward. Here, and throughout this work, we show how one can use model systems to expand the real system around.

Throughout the calculations that are presented, we use linear approximation, i.e. we Taylor expand our charge density. A general form is following,

$$f(x) = f(a) + (x - a)f'(a) + \dots$$

If one wants to stop in some order, say nth order the above equation is no longer exact and one has,

$$f(x) \approx f(a) + (x-a)f'(a) + \cdots + \frac{f^{(n)}(a)}{n!}(x-a)^n \equiv T_n(x) \tag{6}$$

Equation 6 is called the nth partial sum of the Taylor series which is by definition not exact. To have an exact form, we have to introduce the so called the *remainder* term, i.e.

$$f(x) = T_n(x) + R_n(x) \tag{7}$$

If we assume that the function If $f^{(n+1)}(x)$ is continuous on an open interval I that includes a and x, then there is a number c between a and x such that the remainder is [7],

$$R_n(x) = \frac{f^{(n+1)}(c)}{(n+1)!}(x-a)^{n+1}$$

This is called the Lagrange's form of the remainder term. Similarly we also have Cauchy's form as follows

$$R_n(x) = \frac{f^{(n+1)}(c)}{n!}(x-c)^n(x-a)$$

To see the differences between the two methods, let us expand f up to second order in x. The Lagrange method gives

$$f(x) = f(a) + (x-a)f'(a) + \frac{(x-a)^2}{2}f''(\xi_L)\,,$$

where $a \leq \xi_L \leq x$ for $x > a$. Of course, one does not know ξ_L a priori, but at least we know in which interval it lies. The choice of Cauchy is instead

$$f(x) = f(a) + (x-a)f'(a) + (x-a)(x-\xi_C)f''(\xi_C)\,,$$

where $a \leq \xi_C \leq x$. Note that both of these expressions are exact. We use linear approximation for our calculations, i.e. we include only up to the first order terms. Inspired by the approaches of Lagrange and Cauchy on the expansion of functions, we are looking for a first-order term which can give the exact function, i.e. $R_0(x)$. One can already see that, for this specific case, the Cauchy and Lagrange forms become equal. This reads,

$$f(x) = f(a) + (x-a)f'(\xi)\,, \tag{8}$$

where ξ is not necessarily equal to a and it gives the exact result. Moreover, note that ξ can even parametrically depend on x now.

2.1 Linear response expansion

Since our quantity of interest is the charge density (of the real system), let us start by the simplest idea: expanding up to the first order, inspired by Taylor expansions (without Cauchy & Lagrange approach). Since the charge density is a *functional* of the potential, either the external potential or a one-body effective potential coming from an auxiliary system, the expansion is more complex than a simple Taylor expansion.

$$n(\mathbf{r};[v]) \approx n(\mathbf{r};[v_0]) + \int d\mathbf{r}' \chi_0(\mathbf{r},\mathbf{r}',v_0)\Big(v(\mathbf{r}') - v_0\Big) \tag{9}$$

In equation 9, we have the expansion around a function v_0 (which depends on $\mathbf{r}$) up to the first order. The functional derivative in the integral which describes the change in the density with respect to the change in the potential, $\frac{\delta n(\mathbf{r})}{\delta v(\mathbf{r}')}\Big|_{v_0} \equiv \chi_0(\mathbf{r},\mathbf{r}',v_0)$, is referred as the "non-interacting density-density response function". Non-interaction comes from the fact that we take the derivative with respect to the effective potential which is due to the KS auxiliary system of non-interacting electrons. However, we did not gain anything by this approximation since the form of $n(\mathbf{r};[v])$ or $\chi_0(\mathbf{r},\mathbf{r}',v_0)$ is still unknown. However, if we choose to expand the density around a constant potential, we gain a significant simplification in our expansion. This time,

$$n(\mathbf{r};[v]) \approx n^h(v_0) + \int d\mathbf{r}' \chi_0^h(|\mathbf{r}-\mathbf{r}'|,v_0)\Big(v(\mathbf{r}') - v_0\Big) \tag{10}$$

where v_0 (we call this the expansion potential from now on) is constant. This implies that the quantities are in the limiting case of a homogeneous potential (hence the superscript h). Therefore, the zeroth order term reduces to the expression of the non-interacting HEG density with respect to the potential. Moreover, the second term is the well-known Lindhard function with the following expression [8],

$$\chi_0^h(q,v_0) = -\frac{k_F}{2\pi^2}\left\{1 - \frac{Q}{4}\left(1 - \frac{4}{Q^2}\right)\ln\left|\frac{Q+2}{Q-2}\right|\right\} \tag{11}$$

with $k_F = \sqrt{-2v_0}$ and $Q \equiv q/k_F$. The subscript 0 indicates the non-interacting electron gas. This seems easily executable now, and the only problem seems to be the choice of the expansion potential, v_0. We are motivated by LPA and choose to use a different model at every $\mathbf{r}$. This implies that our v_0 is now parametrically dependent on the position, $v_0 \to v_{0\mathbf{r}}$ even though at every $\mathbf{r}$, it is still a constant so that equation 10 holds.

When we choose the expansion potential at each point as the local effective potential at that point, i.e. $v_{0\mathbf{r}} = v(\mathbf{r})$, we obtain the result presented in Figure 3. Compared to the LPA (see Figure 2), we more or less have the same amount of accuracy. The two ears which are exactly mimicking the effective potential (see Figure 1(b)) are not present in the reference density (see Figure 1(a)). This means that the method is unable to effectively adjust the model's behavior to accurately translate it to match the real system. Therefore, a better direction is necessary.

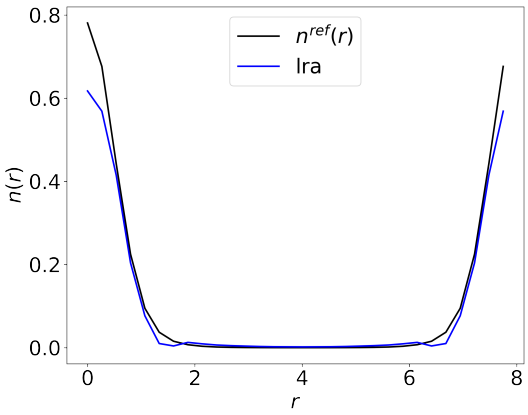

Figure 3: Linear response approximation (LRA) using $v_{0\mathbf{r}} = v(\mathbf{r})$ in comparison to the reference density.

2.2 Motivation from the Cauchy & Lagrange approach

As a next step, we employ the Cauchy & Lagrange approach presented in the beginning of Section 2. If we translate equation 8 to functional realm, we obtain the following modification to our previous expansion,

$$n(\mathbf{r};[v]) = n^h(v_0) + \int d\mathbf{r}' \chi_0^h(|\mathbf{r}-\mathbf{r}'|, \tilde{v}_0)\Big(v(\mathbf{r}') - v_0\Big) \tag{12}$$

where we have the same form as equation 10. The key point is that we are now able to choose to evaluate the derivative, χ_0^h, at an optimal point $\tilde{v}_0 \neq v_0$. Employing this method by getting inspiration from Cauchy & Lagrange (CL), we have to make a choice for v_0, and $\tilde{v}_0$. For this, we have two potential approaches, choosing the same local expansion potential for the zeroth term as before, i.e. $v_0 = v(\mathbf{r})$ and investigating an optimal $\tilde{v}_0$; or choosing the same local expansion potential for the evaluation of χ_0^h, and choosing a constant potential for the zeroth order term. In this study, we opt for the latter approach, noting that our previous investigations into the former approach have yielded promising results (see the Appendix C). Our choice for the constant expansion potential (for the zeroth order term) is intuitive: the average potential, $\bar{v}$, which yields the average number of electrons when plugged into the model system, i.e. $n^h(\bar{v}) = \bar{n}$ where $\bar{n}$ is the average number of electrons in the real system. Following these motivations, our expansion in equation 12 becomes

$$n(\mathbf{r};[v]) = n^h(\bar{v}) + \int d\mathbf{r}' \chi_0^h(|\mathbf{r}-\mathbf{r}'|, v_{0\mathbf{r}})\Big(v(\mathbf{r}') - \bar{v}\Big) \tag{13}$$

with $v_0 = \bar{v}$ and $\tilde{v}_0 = v_{0\mathbf{r}} = v(\mathbf{r})$.

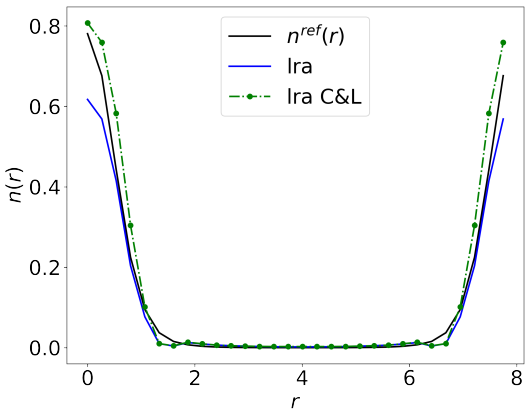

Figure 4: Linear response approximation (LRA) using local v_0 (eqn. 10) and Cauchy & Lagrange method (eqn. 13), in comparison to the reference density.

In Figure 4, we see the results in comparison to our previous expansion (equation 10). By choosing a different point to evaluate the response function, we aim to simulate the higher order terms in the expansion with respect to χ_0^h, equivalent to the idea presented in equation 7. From the results, we observe an improvement in the high density regions with a slight overestimation around where the Helium atoms are placed. Even though this is already a better qualitative description of our system, one needs in principle a robust method which takes a given input and yields a function which mimics the real system rather than the model system. The appearance of two ears in the low density-regime therefore tells us that in order to achieve more robust results, one needs to go beyond. One idea is to go beyond nearsightedness and use non-local expansion potentials; or some other mathematical object which is able make an effective connection between real and model systems. The second idea is to acknowledge the fact that we have been using the non-interacting HEG as our model system and this is already a point that needs to be improved by introducing interactions and expanding by an interacting response function. In the following sections, we examine both approaches and explore how they can be systematically combined to draw insights.

3 Connector Theory (COT)

Motivated by the need to go beyond nearsightedness and linear response expansion, we present a novel theory developed within the group. Connector Theory (COT) is a general approach that provides, in principle, an exact connection between a real system and a model system through the concept of "connector" [5]. By construction, this theory provides a powerful method to reuse tabulated results from these models by introducing a "connector". A connector is a mathematical object that can provide exact values for desired observables in real systems when applied within the model

system. In-detail formalism and some applications can be found in [5], with a short summary in Appendix A.

For simplicity, let us focus now on the local approximations, namely the LPA for our case. In this approximation, LPA replaces the density at each point with that of a HEG with a potential (density) equal to the local potential at that point, i.e.

$$n(\mathbf{r};[v]) \approx n^h(v(\mathbf{r})) \tag{14}$$

Here, one directly approximates the desired quantity from the beginning. Therefore, the systematic improvement of this approximation towards an exact result is not apparent. Instead, if one starts with not an approximation but an exact relation, then this change in point of view allows us to re-write the problem in a more systematic way. Now consider that there is a different potential, which may vary at each point, that, when applied to the model system, produces the exact value as in the real system. Let us call this the "exact connector" and denote it as $v^h_{c\mathbf{r}}$ (superscript h means that this quantity is constant for every point, subscript c is short for "connector").

$$n(\mathbf{r};[v]) = n^h(v^h_{c\mathbf{r}}) \tag{15}$$

Of course, there is no reason for this object to be the same as the local quantity, $v(\mathbf{r})$. In fact, from here it can be seen that LPA becomes only one of the limiting cases of COT where we choose the connector to be the local potential, $v^h_{c\mathbf{r}} = v(\mathbf{r})$ which is a completely nearsighted approach. In reality, the real system exhibits a much more complex behavior, and the general form of the connector shows promise for effectively simulating this complexity [5]. Therefore, the question becomes how to find this connector which gives us the exact results in equation 15. We apply the same approach as Figure A.11, applying the same approximations on both sides of equation 15. This allows us to invert the model and obtain $v^h_{c\mathbf{r}}$. Without approximating both sides, we have $v^h_{c\mathbf{r}} = (n^h)^{-1}(n(\mathbf{r};[v]))$, therefore, it is impossible to solve for the connector since we do not know $n(\mathbf{r};[v])$. Throughout this study, we will use linear response approximation on both sides for consistency.

3.1 Local Connector

Let us try to obtain the charge density functional, $n(\mathbf{r};[v])$ now. Our goal is to linearly expand both sides of the exact connection (equation 15). Noting the expression within the model system,

$$n^h = \frac{[-2v^h]^{3/2}}{3\pi^2} \tag{16}$$

then the exact connection is made,

$$n(\mathbf{r};[v]) = n_h(v^h_{c\mathbf{r}}) = \frac{[-2v^h_{c\mathbf{r}}]^{3/2}}{3\pi^2} \tag{17}$$

Since there is no way to invert this without the knowledge of the real system charge density, we will expand both sides around a homogeneous potential, v_0, in the first order and equate them. Left-hand side reads,

$$n(\mathbf{r};[v]) \approx n_h(v_0) + \int d\mathbf{r}' \chi^h_0(|\mathbf{r}-\mathbf{r}'|, v_0)\Big(v(\mathbf{r}') - v_0\Big) \tag{18}$$

and the right-hand side,

$$n_h(v_h) \approx n_h(v_0) + \left.\frac{dn_h(v_h)}{dv_h}\right|_{v_0} (v_h - v_0) \tag{19}$$

And now we equate both sides to solve for the connector potential. Since we are expanding around a homogeneous function, we get cancellations on both sides which yields,

$$v^h_{c\mathbf{r}} = \left(\left.\frac{dn_h(v_h)}{dv_h}\right|_{v_0}\right)^{-1} \int d\mathbf{r}' \left.\frac{\delta n(\mathbf{r})}{\delta v(\mathbf{r}')}\right|_{v_0} v(\mathbf{r}')$$

noting the derivative of $n_h(v_h)$ is easily computed from equation 16,

$$\left.\frac{dn_h(v_h)}{dv_h}\right|_{v_0} = -\frac{\sqrt{-2v_0}}{\pi^2}$$

Equivalently, this derivative is also the $q \to 0$ behavior of χ^h_0,

$$\left.\frac{dn_h(v_h)}{dv_h}\right|_{v_0} = \chi^h_0(q \to 0, v_0) = \int d\mathbf{r}' \chi^h_0\left(|\mathbf{r}-\mathbf{r}'|, v_0\right)$$

As a result, we obtain the (linear response) connector as,

$$v^h_{c\mathbf{r}} = -\frac{\pi^2}{\sqrt{-2v_0}} \int d\mathbf{r}' \chi^h_0\left(|\mathbf{r}-\mathbf{r}'|, v_0\right) v(\mathbf{r}') = \frac{\displaystyle\int d\mathbf{r}' \chi^h_0\left(|\mathbf{r}-\mathbf{r}'|, v_0\right) v(\mathbf{r}')}{\displaystyle\int d\mathbf{r}' \chi^h_0\left(|\mathbf{r}-\mathbf{r}'|, v_0\right)} \tag{20}$$

This is the linear response connector since our choice of approximation was in the linear regime.

The connector, by its nature, inherits the connection between locality and non-locality and it presents a way to terminate the linear expansion in a clever way . If we compare the LPA ($v^h_{c\mathbf{r}} = v(\mathbf{r})$) to the general form of the connector in equation 20, we realize that the connector behaves as an average around the point of interest for every position. This average is taken by a distribution function which depends on the approximation, χ^h_0 for our case. Therefore, the connector takes into account the dependence on the environment, $v(\mathbf{r}')$, at every $\mathbf{r}$, and the ingredient $\chi^h_0(|\mathbf{r}-\mathbf{r}'|, v_0)$ purely comes from the model.

From equation 20, one can see that the only ingredient to compute the connector is the expansion potential, v_0. This choice is crucial in order to improve the connector and one of the goals is to make this choice of the initial point systematic. For now, we choose the same starting potential, i.e. the connector expands around the local potential, $v_{0\mathbf{r}} = v(\mathbf{r})$. In the next chapters, the validity and improvement of this choice will be discussed. Finally, after obtaining the connector, we plug $v^h_{c\mathbf{r}}$ into equation 17 to obtain the density.

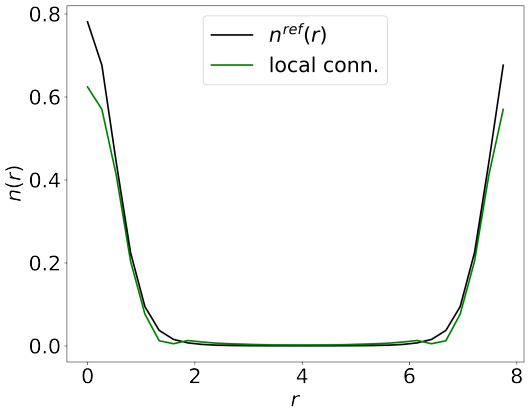

Figure 5: Linear response connector using local v_0 in eqn. 20 in comparison to the reference density.

If we compare Figure 5 to Figure 3, we see that the local connector does not provide a significant improvement. However, thanks to the systematic formulation of the connector, we are free to improve how we calculate $v^h_{c\mathbf{r}}$.

3.2 Bilocal Connector

As discussed at the end of Section 2.2, we propose two ways for more accurate descriptions within expansion around models. In this section, we investigate the first approach: introducing non-locality. At this point, this choice becomes a natural step forward within the connector formalism since the connector provides a way to exploit the non-locality. Moreover, introducing this non-locality will be equivalent to using the

CL approach within linear response expansion in Section 2.2, since we have again a terminator different than the zeroth order. To go beyond the local v_0, we are inspired by the general form of the response function, $\chi(\mathbf{r}, \mathbf{r}')$. This already suggests non-locality, thus; we abandon our choice of $v_0 = v(\mathbf{r})$ and instead use an expansion potential that is non-local. For this, the simplest choice would be a bilocal expansion potential, i.e. $v_0 = \frac{v(\mathbf{r})+v(\mathbf{r}')}{2}$. Thus, we introduce bilocality by the following modifications,

$$\chi_0^h(|\mathbf{r}-\mathbf{r}'|, v_0) \longrightarrow \chi_0^h\left(|\mathbf{r}-\mathbf{r}'|, \frac{v(\mathbf{r})+v(\mathbf{r}')}{2}\right)$$

However, this modification is not so straightforward. In equation 20, we easily notice that in the prefactor of the integral, we have the v_0 outside the integral, therefore; it is meaningless to use a non-local potential. As a solution to that and for the sake of approximating the model and the real system in an equivalent way, we use the following expansion potential for the model

$$v_{\mathbf{r}\mathbf{r}_c} = \frac{v(\mathbf{r}) + v^h_{c\mathbf{r}}}{2}$$

These modifications lead us to the following connector,

$$v^h_{c\mathbf{r}} = -\frac{\pi^2}{\sqrt{-2v_{\mathbf{r}\mathbf{r}_c}}} \int d\mathbf{r}' \chi_0^h\Big(|\mathbf{r}-\mathbf{r}'|, v_{\mathbf{r}\mathbf{r}'}\Big) v(\mathbf{r}') \tag{21}$$

where $v_{\mathbf{r}\mathbf{r}'} = \frac{v(\mathbf{r})+v(\mathbf{r}')}{2}$. Note that now, at each point $\mathbf{r}$, v_0 is a function of $\mathbf{r}'$ and we consider a broader neighborhood in real space which means we are dealing with less-nearsightedness. Figure 6(a) shows the result.

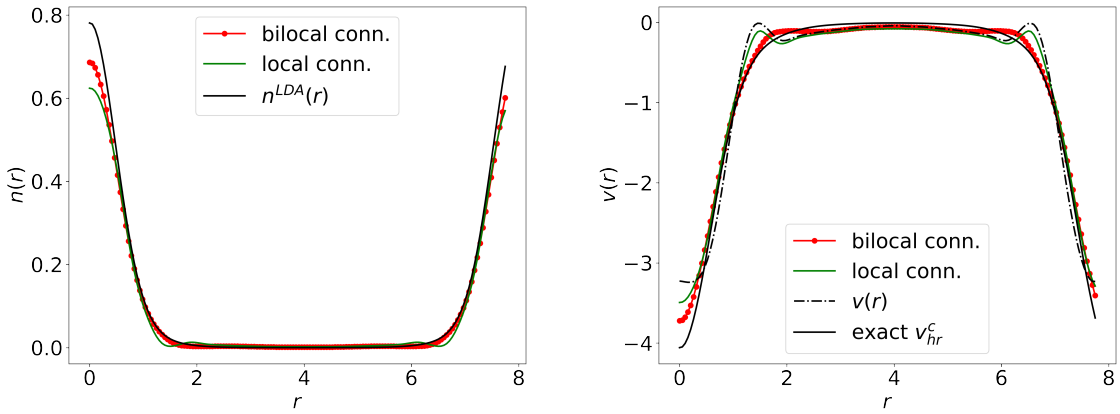

Figure 6: **Left:** Linear response connector using local (green) versus bilocal v_0 (red dotted) in eqn. 20 in comparison to the reference density. **Right:** Corresponding connectors in comparison to the local effective potential (dashdotted black) and the exact connector (solid black). More data points were used for demonstration purposes.

We see that we now have a significant improvement in the charge density. In our previous results, we had two ears around $r = 1.5a_0$ and $r = 6.5a_0$ that were coming from the behavior of the effective potential. Due to averaging between two distinct points, our bilocal connector is able to average out while additionally improving the high-density regime. This means that the connector is now able to interpolate between locality (LPA) and non-locality (towards the real solution). This is demonstrated in Figure 6(b). By using connector, one uses systematically the effective potential (dashdotted black curve) and generates a new connector which is designed to get closer to the exact connector (solid black curve, calculated by inverting the reference density from eqn. 16). Additionally we see that the bilocal connector is much more successful than the local connector in terms of resembling the exact connector. Moreover, we observe that by employing the connector approach with a non-interacting gas model, we are able to achieve a remarkable qualitative description of a system that is highly far away from a homogeneous one. The success of this method highlights the robustness and versatility of the connector theory. Even for systems that deviate considerably from the idealized homogeneous electron gas, the connector can effectively capture the essential physics, providing a reliable approximation to the exact solution.

4 Going beyond: expansion around the interacting gas

In the previous chapter, we explored the advancements achievable by extending the concept of locality through the use of bilocal connectors. This approach demonstrated significant improvements in the precision of approximations and predictions within the framework of COT. However, to fully harness the potential of these mathematical tools and address the complex nature of many-body systems, it is imperative to incorporate the interactions between electrons within the model more explicitly. This will not only describe our system more accurately, but also will enable us to surpass using auxiliary systems such as Kohn-Sham electrons within the framework of LDA-DFT (which we assume gives us the "exact" density) that already has certain amount of error. In other words, we will expand our system with respect to the external potential, $v_{\text{ext}}(\mathbf{r})$ (which is known without approximations), and not the effective potential. Therefore, we are no longer restricted by the limitations coming from DFT.

We begin by re-visiting our linear expansion for the charge density in the non-interacting HEG case. We have been denoting the effective potential as $v(\mathbf{r})$ and this was actually the Kohn-Sham potential coming from DFT calculations. This is a non interacting auxiliary system which allowed us to use the non-interacting response function. If we want to include interactions, we therefore need to expand the density with respect to the external potential, $v_{\text{ext}}(\mathbf{r})$, rather than the KS potential. Therefore we obtain

$$n(\mathbf{r};[v_{\text{ext}}]) \approx n^h(v_0) + \int \chi^h_{\text{LDA}}(\mathbf{r}-\mathbf{r}', v_0)\big(v_{\text{ext}}(\mathbf{r}') - v_0\big)d\mathbf{r}' \tag{22}$$

where the response function of the interacting electron gas is defined by

$$\left.\frac{\delta n(\mathbf{r})}{\delta v_{\text{ext}}(\mathbf{r}')}\right|_{v_0} \equiv \chi^h_{\text{LDA}}(|\mathbf{r}-\mathbf{r}'|, v_0) \tag{23}$$

The reason why we have a subscript denoting LDA is because our reference density is actually calculated within LDA. Therefore, its response with respect to v_{ext} will be within the LDA picture, hence χ^h_{LDA}. Before starting with calculations, we have to address some intricate points when changing our picture towards the interacting case. Firstly, the zero order term in equation 22 does not have the same form as in the previous cases. In fact $n^h(v)$ now describes the interacting charge density of the gas, whose form with respect to the potential is not as straightforward. In the non-interacting case, we have the following relation for the chemical potential,

$$\mu = \frac{k_F^2}{2} + v \implies k_F = \sqrt{2(\mu - v)} \tag{24}$$

Which correspond to our previous calculations if one fixes $\mu = 0$. However, when we have interactions the situation is different,

$$\mu = \frac{k_F^2}{2} + v_{\text{ext}} + v_{\text{xc}}[n] = \frac{1}{2}(3\pi^2 n)^{2/3} + v_{\text{ext}} + v_{\text{xc}}[n] \tag{25}$$

In this case, we realize the implicit dependence of the exchange-correlation potential of the gas on the density. Fortunately, the numerically exact solution of v_{xc} and its parametrization is given by [9, 10]. Therefore, we have numerical access to the solution of equation 25, i.e. $n(v_{\text{ext}})$. The difference can be observed in Figure 7(a).

Secondly, the argument v_0 in χ^h_{LDA} means that we are using the gas that has the same *interacting* density now, therefore we need to modify k_F in equation 11 accordingly. With these modifications, we can now look at how to calculate the expansions thanks to the numerical solution of equation 25.

Let us observe equation 23. Of course, the "interaction" that we introduce is only in the LDA level (since our target density is the LDA charge density). Since we already know the (exact) external potential, the only ingredient to calculate is $\chi^h_{\text{LDA}}(\mathbf{r}-\mathbf{r}', v_0)$ which is the functional derivative of the LDA charge density with respect to the external potential evaluated at a homogeneous potential. In other words, this response function is the response of the interacting electron gas which can be obtained from a Dyson-like equation,

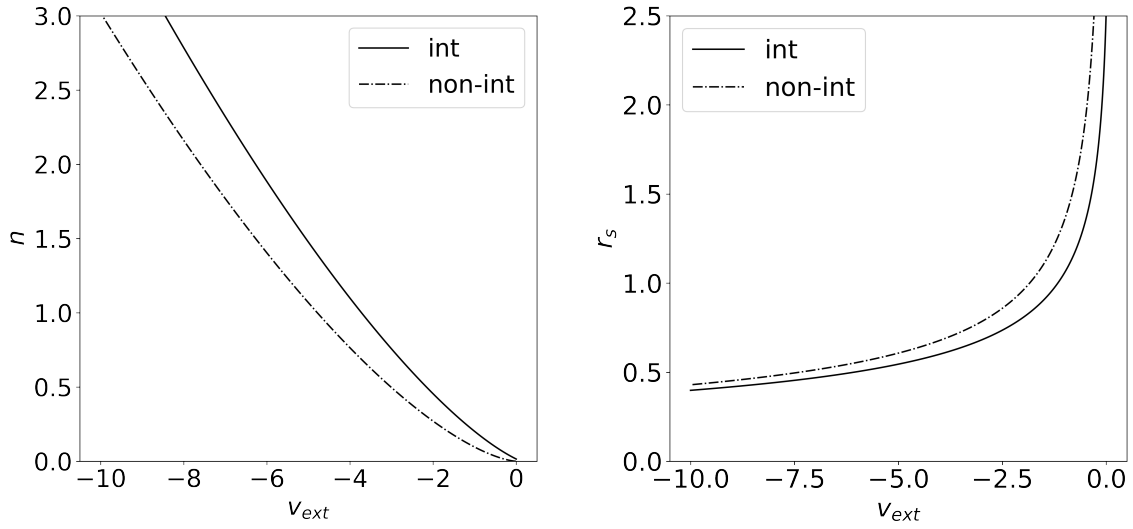

Figure 7: **Left:** Charge density (left) and the electron gas parameter $r_s = (\frac{3}{4\pi n})^{1/3}$ (right) as a function of v_{ext} for the interacting (solid) and non-interacting (dashed) electron gas.

$$\chi^h_{\text{LDA}}(q) = \chi^h_0(q) + \chi^h_0(q)(v_q + f^{\text{LDA}}_{\text{xc}})\chi^h_{\text{LDA}}(q) \tag{26}$$

$$= \frac{\chi^h_0(q)}{1 - \chi^h_0(q)(v_q + f^{\text{LDA}}_{\text{xc}})} \tag{27}$$

where $v_q = 4\pi/q^2$ is the Coulomb interaction in the reciprocal space, $f^{\text{LDA}}_{\text{xc}} = f_{\text{xc}}(q \to 0)$ is the exchange-correlation kernel which is numerically exact thanks to quantum Monte Carlo calculations [11].

It is easy to verify that, due to the Coulomb interaction, $\chi^h_{\text{LDA}}(q)$ quickly goes to zero as $q \to 0$. This is problematic, since when we use the connector approach, we divide by this value, i.e.

$$v^h_{c\mathbf{r}} = \int \frac{\chi^h_{\text{LDA}}(q, v_0)}{\chi^h_{\text{LDA}}(q \to 0, v_0)} v_{\text{ext}}(q) e^{iq|\mathbf{r}-\mathbf{r}'|} dq \tag{28}$$

Moreover, we expect that our real system converges to the model in the homogeneous limit, however within linear response (of a homogeneous system) we have

$$n(v) = n(v_0) + \chi^h_{\text{LDA}}(q \to 0, v_0)(v - v_0) = n(v_0)$$

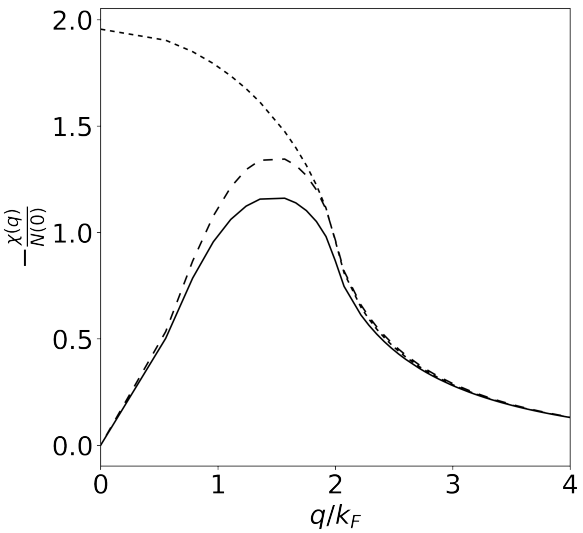

Figure 8: Behavior of the three dimensional static density response function in RPA (full line) and LDA (long dashed line) for a 3D electron gas. The short dashed line reproduces the corresponding non-interacting (Lindhard) function.

which shows a disappearance of the linear term due to the $\mathbf{q} \to 0$ behavior (see Figure 8) which this does not appear in our real system.

4.1 Macroscopic contribution to the linear expansion

To understand why we encounter this problem, let us focus once again on the linear expansion since it lies at the heart of our connector approximations. Consider the possible two directions one can pursue. We have first the usual linear expansion around LPA from section 2.1, i.e.

$$n(\mathbf{r};[v_{\text{ext}}]) \approx n^{\text{h}}(v_{0\mathbf{r}}) + \int \chi^{h}_{\text{LDA}}(\mathbf{r}-\mathbf{r}', v_{0\mathbf{r}})\big(v_{\text{ext}}(\mathbf{r}') - v_{0\mathbf{r}}\big)d\mathbf{r}' \tag{29}$$

with $v_{0\mathbf{r}} = v_{\text{ext}}(\mathbf{r})$. Additionally, as introduced in section 2.2, we have the other form inspired by Cauchy & Lagrange, i.e.

$$n(\mathbf{r};[v_{\text{ext}}]) \approx n^{\text{h}}(\bar{v}) + \int \chi^{h}_{\text{LDA}}(\mathbf{r}-\mathbf{r}', v_{0\mathbf{r}})\big(v_{\text{ext}}(\mathbf{r}') - \bar{v}\big)d\mathbf{r}' \tag{30}$$

where $\bar{v} = n_h^{-1}(\bar{n})$ with $\bar{n}$ being the average number of electrons in the real system. The problem arises when one directly calculates these two expressions within the interacting HEG case, without taking into account $\chi^{h}_{\text{LDA}}(q \to 0) = 0$.

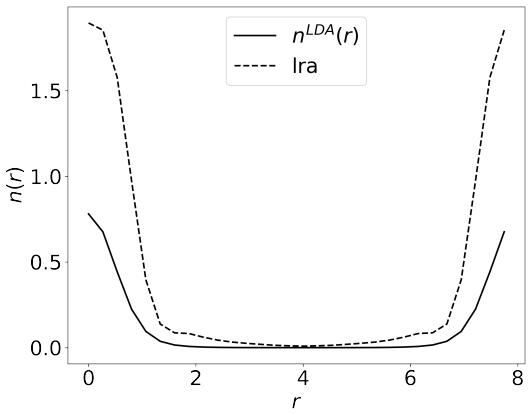

Figure 9: Charge density calculated using equation 29

As one can see, the result presented in Figure 9 is not satisfactory. In fact, we can intuitively infer that this phenomenon is the manifestation of what we encountered before coming from the $\chi^h_{\text{LDA}}(q \to 0)$ term in equation 29. In this section, we will show that this behavior of the interacting response function only accounts for microscopic density variations and there is an additional macroscopic contribution arising when we carefully expand the charge density.

To understand why we encounter this issue (and why it was not present in our previous expansions using the non-interacting HEG) let us rewrite our problem to have a clearer framework. Since we are modelling an inhomogeneous system by a homogeneous model (HEG), we need to have a clear distinction when we evaluate by a homogeneous model/variable or inhomogeneous model/variable. Now let us consider that our potential felt by electrons is combination of a homogeneous potential and variations, i.e.

$$v_{\text{ext}}(\mathbf{r}) = \bar{v} + \Delta v(\mathbf{r})$$

For convenience, we will choose $\bar{v}$ so that it yields the correct electron number in the model, i.e. $n^h(\bar{v}) = \bar{n} = 2$. In other words, we consdier the following notation change,

$$n(\mathbf{r}; [v_{\text{ext}}]) \equiv n(\mathbf{r}; [\bar{v}, \Delta v])$$

Where Δv is a function and $\bar{v}$ is a constant. This is a well known method in solid state physics of infinite systems. Note that when we have no variations on the potential we recover the expression in the HEG, i.e. $n(\bar{v}, 0) = n^h(\bar{v})$.

Now we can treat each term (homogeneous and inhomogeneous) carefully and turn our previous approach into two expansions: one as a function of $\bar{v}$ and one as a functional

of $\Delta v(\mathbf{r})$. Note that $n(\bar{v}, 0) = \bar{n}$. If we choose to expand around $(\bar{v}, \Delta v) = (v_0, 0)$ the expansion (in the most general form) can be written now as,

$$n(\mathbf{r}; [\bar{v}, \Delta v]) = n(v_0, 0) + \frac{\partial n}{\partial \bar{v}}\Big|_{v_0} (\bar{v} - v_0) + \frac{1}{2}\frac{\partial^2 n}{\partial \bar{v}^2}\Big|_{v_0} (\bar{v} - v_0)^2 + \dots$$
$$+ \int \chi(\mathbf{r}, \mathbf{r}'; v_0, \Delta v = 0)\Delta v(\mathbf{r}')d\mathbf{r}' + \dots \tag{31}$$

With this form, the problem becomes clear. If we choose local v_0 and stop in the zeroth term in the first line, then equation 31 becomes equation 29 which is equivalent of expansion around local v_0 and leads to an overestimation from Figure 9. Since we do not include further terms in the expansion, we therefore lack a macroscopic contribution. Instead, if one does not stop in the zeroth order for the Taylor expansion in equation 31 and goes up to all orders, we recover equation 30. In other words, equation 29 is just a non-converged version of equation 30 (it was not the case for non interacting HEG since $\chi^h_{\mathrm{LDA}}(q \to 0) \neq 0$). This time, we now have the macroscopic correction coming from the higher order terms in the first line of equation 31 which are clearly nonzero

$$\frac{\partial n}{\partial \bar{v}}\Big|_{\bar{v}=v_0} \neq \chi^h_{\mathrm{LDA}}(q \to 0, v_0)$$

The result (with the addition of macroscopic contributions which corresponds to equation 30) is presented in Figure 10.

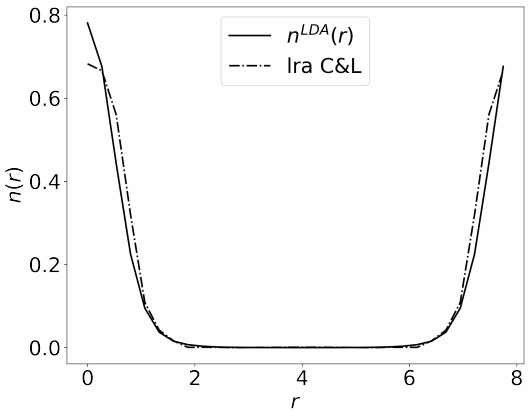

Figure 10: Charge density calculated using equation 30

But why did we not encounter this before? Let us now investigate the expansion around the non-interacting HEG (using χ^h_0). In this case we have a nonzero macroscopic contribution due to the nonzero behavior of $\chi^h_0(q \to 0, v_0)$. Thus, we did not need to

go further to include all orders in the expansion of the first line of equation 31 (even though it can be easily doable) since the macroscopic contribution is already nonzero. Therefore, we conclude by stating the importance of the macroscopic contribution when including the interaction effects in the model.

Comparing Figure 10 with Figure 4, we see the the significance of the inclusion of interaction effects. We notice that our method now more accurately replicates the real system, even when the input potential may not directly correlate with its shape. The two ears apparent in both external and Kohn-Sham potentials are taken care of when we introduce interactions. This is a quite promising direction for applying this approach on more realistic materials.

5 Conclusion

In this work, we studied methodologies for effectively using model systems to describe real system properties, specifically for the charge density. Motivated by the Local Density Approximation, we showed how one can start from a local approximation (Section 1.4), move beyond by expanding around a model (Section 2), and even exactify it by using the Connector Theory (Section 3). Throughout our studies, we used the non-interacting homogeneous electron gas as our model. Our results showed the possibility of obtaining qualitative satisfying results without solving the Schrödinger equation. In Section 4, we showed how one can even go beyond and use the interacting homogeneous electron gas as model. Our latest results confirm that our method imitates the real system much more accurately which may have significant implications for applications.

All calculations present in this study are computationally very affordable since we do not diagonalize the Hamiltonian. Moreover, after tabulating the model system once, χ_0^h or χ_{LDA}^h for instance, one can reuse these model results for any kind of system without having any additional computation time. The only ingredient that one needs is the choice of the expansion potential v_0 since every system needs a specific approach.

5.1 Future Work

Cubic Helium is not an easy system. The rapidly changing nature of the density around the atoms makes our calculations difficult to capture its behavior. Nevertheless, the results are already astonishingly good.

Our next step would be to employ the connector since with interactions, equation 20 transforms into,

$$v_{h\mathbf{r}}^c = \bar{v} + \frac{1}{\frac{\partial n}{\partial \bar{v}}\big|_{v_0}} \int d\mathbf{r}' \chi\left(\mathbf{r}, \mathbf{r}'; v_0, \Delta v = 0\right) \Delta v(\mathbf{r}') \tag{32}$$

after our notation change in Section 4.1. From here, we would like to apply our methods

for more realistic systems in order to see whether our approximation could already be used for certain classes of materials. Our immediate goal would be to investigate charge densities of Silicon and Sodium Chloride since the exact densities of these materials are calculated recently [12]. To achieve this, one needs to go beyond the DFT calculations. Fortunately, our latest results shows promise into this direction. In fact, we are now able to use the (numerically) exact form of the response function since it is calculated by quantum Monte-Carlo calculations.

A Connector Theory: Formalism

Generally, the desired observable in a given system is expressed as $O[x;Q^R]$, where Q is a function of x and O is a functional. In most cases, this functional is impossible to calculate; therefore, the approximations are applied directly to O. In the case of the LDA, for instance, the exchange-correlation potential $v_{\rm xc}(\mathbf{r},[n])$ is approximated by HEG as the model system,

$$v_{\rm xc}(\mathbf{r},[n]) \approx v^h_{xc}(n^h_{\mathbf{r}})$$

where $n^h_{\mathbf{r}} = n(\mathbf{r})$, meaning that the xc potential at point $\mathbf{r}$ is taken from the same point in the HEG. This implies that the computation of the xc potential, $v^h_{xc}(n^h_{\mathbf{r}})$, which belongs to the model system is only to be made once. Then, one could apply this result to approximate any real system. But this choice of local density as a connector can be generalized.

If one is certain that the solutions of v^h_{xc} span all the possible solutions of the real system, this means that it is possible to find a better connector $n^h_{\mathbf{r}}$ that yields more accurate -or even exact- results for the real system. Then, once this connector is tabulated, it can be used for the approximations of any real systems.

In the general formalism, the exact implication of the connector theory is the following equality,

$$O[x;Q^R] = O[x;Q^c_x] \tag{33}$$

where Q^R lies in the real domain and Q^c lies in the model domain (HEG for instance). The theory assumes that there exists an exact connector, Q^c_x, which can be different at each x, that fulfills the equality above. If we choose the model domain such that it can be described by one effective parameter, we have $O[x;Q^c_x] \to \mathcal{O}_x(\mathcal{Q}^c_x)$. In the HEG, for instance, we can describe the system with its number density, n_h. Thus, the expression for the exact connector, $\mathcal{Q}^c_x$ is formally solved,

$$\mathcal{Q}^c_x = \mathcal{O}^{-1}_x\left(O[x;Q^R]\right) \tag{34}$$

After obtaining the connector, one plugs it into eqn. (5),

$$O[x;Q^R] = \mathcal{O}_x(\mathcal{Q}_x^c) \tag{35}$$

In fact, the transition from eqn. (6) to eqn. (7) is not so simple and direct. The argument in the RHS of eqn. (6) -the observable of the real system- is principally not known. Thus, one needs to make approximations to both sides of eqn. (5). This implies that we would solve for an approximate connector,

$$\mathcal{Q}_x^{c,\text{approx}} = (\mathcal{O}_x^{\text{approx}})^{-1}\left(O^{\text{approx}}[x;Q^R]\right) \tag{36}$$

$$O[x;Q^R] \approx \mathcal{O}_x(\mathcal{Q}_x^{c,\text{approx}}) \tag{37}$$

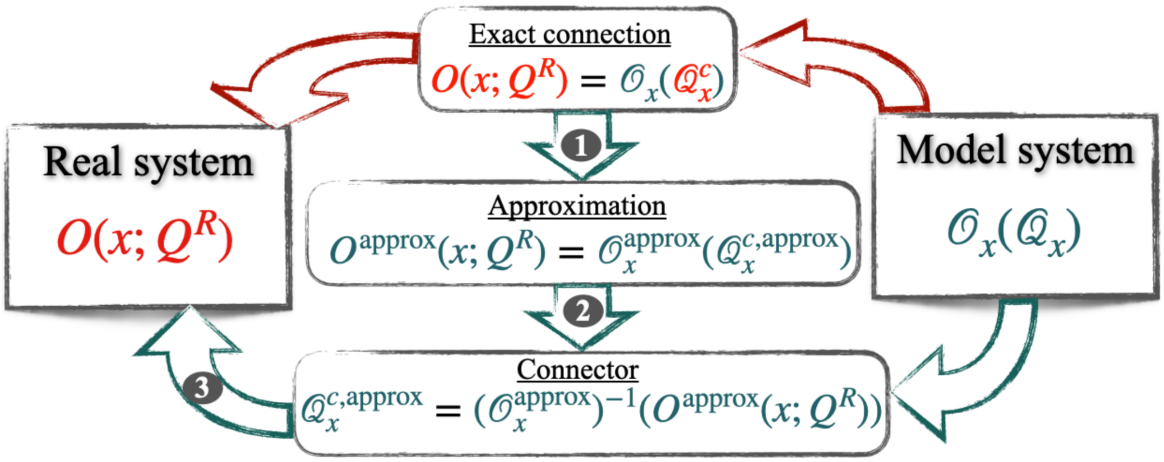

Figure 11: Schematic summary of the connector approach. Green and red colors represent what is known and unknown, respectively. Since $\mathcal{Q}_x^c$ is not known, we apply approximation to the exact connection. After obtaining the approximate connector, $\mathcal{Q}_x^{c,\text{approx}}$, we plug it into the model system. Figure adopted from [?].

The success of COT comes from the fact that when the same approximation is applied to both sides, there is a significant error cancellation in eqn. (8). In fact, the connector theory becomes exact in two limits: when the approximation becomes increasingly good, and when the domain of the model system tends toward that of the real system. Using a connector is expected to yield more accurate results than applying direct approximations to $O[x;Q^R]$ with no additional computational cost.

B Derivation of the Lindhard Function for the 3D Electron Gas

In this section, I present the derivation of the real-space Lindhard function $\chi_0(r)$. The Lindhard function describes the density–density response of a system in the linear regime. In our calculations, we are interested in this response of the homogeneous electron gas. The one-spin density and the DOS for the 3D HEG are given as,

$$n_\sigma = \frac{k_F^3}{6\pi^2}$$
$$\rho_{F\sigma} = \frac{k_F}{2\pi^2}$$

and in the static case ($\omega \to 0$), the one-spin Lindhard function is,

$$\chi_{0\sigma}(q) = \frac{1}{L^3} \sum_{\mathbf{k}} \frac{n_{\mathbf{k}\sigma} - n_{\mathbf{k}+\mathbf{q}\sigma}}{\epsilon_{\mathbf{k}\sigma} - \epsilon_{\mathbf{k}+\mathbf{q}\sigma}} \tag{38}$$

Carrying out this calculation (done in [8]), we obtain,

$$\chi_{0\sigma}(q) = -\rho_{F\sigma} \left[\frac{1}{2} + \frac{Q^2 - 4}{8Q} \ln \left| \frac{Q-2}{Q+2} \right| \right] \tag{39}$$

where $Q \equiv q/k_F$. Since our system is isotropic, the result only depends on q, rather than $\mathbf{q}$. The real space Lindhard function is calculated as Fourier transforming $\chi_0(q)$,

$$\chi_{0\sigma}(r) = \int_{-\infty}^{\infty} \frac{dq}{(2\pi)^3} \chi_{0\sigma}(q) e^{iqr} \tag{40}$$

Carrying out this calculation (done in [8]), we obtain,

$$\chi_{0\sigma}(r) = 12\pi n_\sigma \rho_{F\sigma} \frac{\sin(2k_F r) - 2k_F r \cos(2k_F r)}{(2k_F r)^4} \tag{41}$$

defining,

$$g(x) = \frac{x\cos x - \sin x}{x^4}$$

and plugging in the expressions for n_σ, $\rho_{F\sigma}$, we obtain

$$\chi_{0\sigma}(r) = \frac{k_F^4}{\pi^3} g(2k_F r)$$

Finally, noting that

$$\chi_0(r) = \chi_{0\uparrow}(r) + \chi_{0\downarrow}(r)$$

we obtain the Lindhard function in real space as,

$$\chi_0(r) = \frac{2k_F^4}{\pi^3} g(2k_F r) \tag{42}$$

C Optimizing v_0: exact solution from the HEG

As stated in the first chapters, we want to find systematic ways to improve our approximations. For this, we focus on how to optimize the expansion potential, v_0 in this chapter. We believe that even a qualitative direction on towards where one needs to modify the expansion potential could be a promising improvement for our results.

Recalling equation 12,

$$n(\mathbf{r}; [v]) = n^h(v_0) + \int d\mathbf{r}' \chi_0^h(|\mathbf{r} - \mathbf{r}'|, \tilde{v}_0)\Big(v(\mathbf{r}') - v_0\Big) \tag{43}$$

Our aim is to seek for $\tilde{v}_0$ that gives the exact result. For this, we have to solve for this expansion potential at every $\mathbf{r}$, however, the analytical solution is impossible due to the explicit form of the Lindhard function. Fortunately, we can benefit from our usual inspiration and use the electron gas as our basis.

For the (noninteracting) gas,

$$n^h(v) = \frac{k_F^3}{3\pi^2} = \frac{(-2v)^{3/2}}{3\pi^2} \tag{44}$$

applying linear expansion around v_0,

$$n^{\text{lin}}(v) = n^h(v_0) + (v - v_0)\chi_0(q \to 0, \tilde{v}_0) \tag{45}$$

here, we have a simple expression for the $\chi_0(q \to 0, \tilde{v}_0)$ which is given as,

$$\chi_0(q \to 0, \tilde{v}_0) = -\frac{\pi^2}{\sqrt{-2\tilde{v}_0}} \tag{46}$$

Thus, it is possible to obtain the optimal expansion parameter for the derivative, i.e. $\tilde{v}_0$. Plugging eqn. 46 into eqn. 45, we obtain

$$\tilde{v}_0 = -\frac{1}{2}\left[\frac{(-2v_0)^{3/2} - (-2v)^{3/2}}{3(v - v_0)}\right]^2 \tag{47}$$

Now, we can use this optimum expansion for the gas and plug it in the real system, equation 12. Further, if we choose $v_0 = v(\mathbf{r})$, the previous expression becomes,

$$\tilde{v}_{0\mathbf{r}\mathbf{r}'} = -\frac{1}{2}\left[\frac{\Big(-2v(\mathbf{r})\Big)^{3/2} - \Big(-2v(\mathbf{r}')\Big)^{3/2}}{3v(\mathbf{r}') - 3v(\mathbf{r})}\right]^2 \tag{48}$$

Finally, we can now use this expression for our real system, i.e. equation 12. All we need to do is to plug in, at each point, equation 48 into the argument of χ_0.

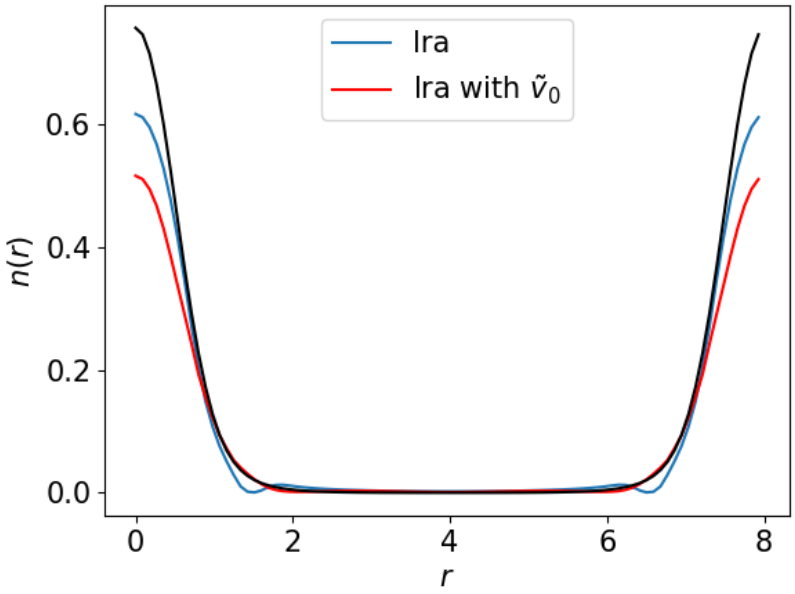

Figure 12: Charge densities using direct linear response with $v_0 = v(\mathbf{r})$ (blue line) and $v_0 = \tilde{v}_{0\mathbf{r}\mathbf{r}'}$ (red line) compared to the reference density (black).

Figure 12 shows the analysis on the direct linear approximation. The blue curve represents the usual expression where $v_0 = v(\mathbf{r})$ (see equation 20). Even though it somewhat performs satisfactory in the high density regime, it fails in the low density regime with the formation of two small peaks which are due to behavior of the local potential. These two peaks that appear in the potential, however, should not effect the result (see the black curve in Figure 12).

The red curve on the other hand, represents the modified direct linear approximation, i.e. eqn. (12). Here, we modify the v_0 to $\tilde{v}_0$ on the derivative term, i.e. inside the expression of χ_0. Our choice of $\tilde{v}_0$ is inspired from that of the homogeneous electron gas given by equation (48). With this approximation, one gains a significant improvement

in the low-density regime while losing accuracy in the high-density regime. Our main objective was to exploit the properties of the electron gas to simulate the reference density. And we can easily see that the modified version of the linear approximation is able make the density qualitatively better, and it is therefore a promising route.

C.1 $\tilde{v}_0$ for the connector

In this section, we extend the previous motivation to the connector calculations. Taking inspiration from the modification $v_0 \to \tilde{v}_0$, we modify the local connector as following,

$$v^c_{h\mathbf{r}} = \frac{\int d\mathbf{r}' \chi_0 \left(|\mathbf{r} - \mathbf{r}'|, \tilde{v}_{0\mathbf{r}\mathbf{r}'}\right) v(\mathbf{r}')}{\int d\mathbf{r}' \chi_0 \left(|\mathbf{r} - \mathbf{r}'|, \tilde{v}_{0\mathbf{r}\mathbf{r}'}\right)} \tag{49}$$

where $\tilde{v}_0$ is the same expression as equation (48). The result with the comparison to the local connector, i.e. $\tilde{v}_0 = v(\mathbf{r})$ is shown in the Figure 13.

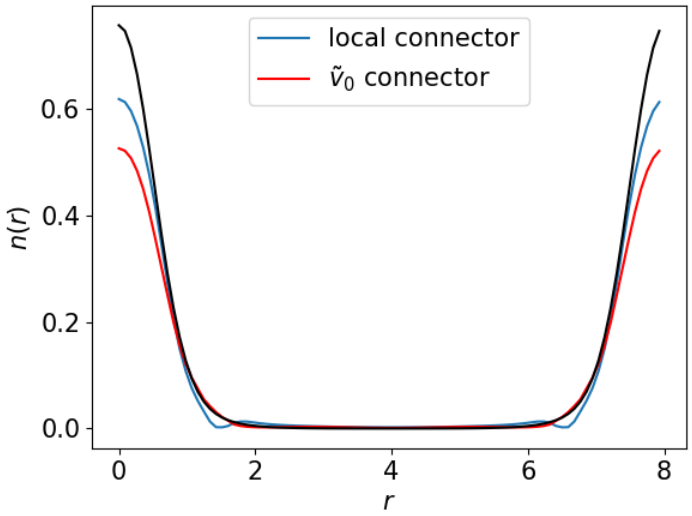

Figure 13: Charge densities using local connector: expansion potential directly from the local potential (blue line) and from $v_0 = \tilde{v}_{0\mathbf{r}\mathbf{r}'}$ (red line).

One can easily notice that the two figures, 12 and 13 are very similar to each other (see the red curves). The reason for this can be justified by the fact that the local connector and the direct linear approximation yields very similar results for the charge density of Helium (the blue curves in Figures 12 and 13). Therefore, previously mentioned remarks for the linear approximation holds for the local connector as well. However, knowing its success for the bilocal case, we can even modify the equation (49) to include

the connector in the denominator to have a self-consistent scheme (previously denoted as *bilocal* $\boldsymbol{rr}_c$). We propose the following modification in the denominator of equation (49),

$$v^c_{h\mathbf{r}} = \frac{\int d\mathbf{r}' \chi_0 \left(|\mathbf{r} - \mathbf{r}'|, \tilde{v}_{0\mathbf{r}\mathbf{r}'}\right) v(\mathbf{r}')}{\int d\mathbf{r}' \chi_0 \left(|\mathbf{r} - \mathbf{r}'|, \tilde{v}_{0\mathbf{r}\mathbf{r}_c}\right)} \tag{50}$$

where

$$\tilde{v}_{0\mathbf{r}\mathbf{r}_c} = -\frac{1}{2}\left[\frac{\Big(-2v(\mathbf{r})\Big)^{3/2} - \Big(-2v^c_{h\mathbf{r}}\Big)^{3/2}}{3v^c_{h\mathbf{r}} - 3v(\mathbf{r})}\right]^2$$

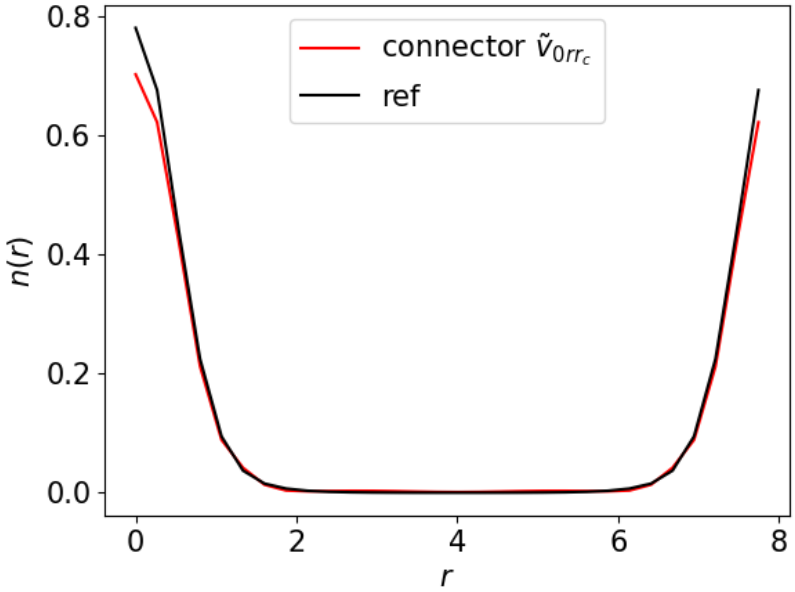

Figure 14: Charge densities using local connector: expansion potential directly from the local potential (blue line) and from $v_0 = \tilde{v}_{0\mathbf{r}\mathbf{r}'}$ (red line).

Inspecting Figure 14, we notice how the modification in v_0 can approach to the exact result significantly. For this, we are interested in systematic methods to treat v_0. Namely, we want to be able to control the expansion potential in certain parts in real space to obtain more accurate charge densities.

References

[1] N. Marzari, A. Ferretti, and C. Wolverton, "Electronic-structure methods for materials design," *Nature Materials*, vol. 20, pp. 736–749, June 2021.

[2] P. Coleman, *Introduction to Many-Body Physics*. Cambridge University Press, 1 ed., Nov. 2015.

[3] W. Kohn, "Nobel Lecture: Electronic structure of matter—wave functions and density functionals," *Reviews of Modern Physics*, vol. 71, pp. 1253–1266, Oct. 1999.

[4] W. Kohn, "Density Functional and Density Matrix Method Scaling Linearly with the Number of Atoms," *Physical Review Letters*, vol. 76, pp. 3168–3171, Apr. 1996.

[5] M. Vanzini, A. Aouina, M. Panholzer, M. Gatti, and L. Reining, "Connector theory for reusing model results to determine materials properties," *npj Computational Materials*, vol. 8, p. 98, May 2022.

[6] X. Gonze, "A brief introduction to the ABINIT software package," *Zeitschrift für Kristallographie - Crystalline Materials*, vol. 220, pp. 558–562, May 2005.

[7] J. Stewart, *Calculus: Concepts and Contexts*. Pacific Grove, CA: Brooks/Cole Pub. Co., 1998.

[8] G. Giuliani and G. Vignale, *Quantum Theory of the Electron Liquid*. Cambridge University Press, 1 ed., Mar. 2005.

[9] D. M. Ceperley and B. J. Alder, "Ground State of the Electron Gas by a Stochastic Method," *Physical Review Letters*, vol. 45, pp. 566–569, Aug. 1980.

[10] J. P. Perdew and A. Zunger, "Self-interaction correction to density-functional approximations for many-electron systems," *Physical Review B*, vol. 23, pp. 5048–5079, May 1981.

[11] S. Moroni, D. M. Ceperley, and G. Senatore, "Static Response and Local Field Factor of the Electron Gas," *Physical Review Letters*, vol. 75, pp. 689–692, July 1995.

[12] S. Chen, M. Motta, F. Ma, and S. Zhang, "*Ab Initio* electronic density in solids by many-body plane-wave auxiliary-field quantum Monte Carlo calculations," *Physical Review B*, vol. 103, p. 075138, Feb. 2021.